DOI: 10.31401/WS.2024.proc.03

Proceedings of
the Sixteenth Workshop "Solar Influences on the Magnetosphere, Ionosphere and Atmosphere"
June, 2024

Temporal Variation of 10.7 cm Solar Radio Flux and Selected Cosmic, Geomagnetic, and Interplanetary Indicators during Solar Cycle 24

Özgüç A.[1], Kilcik A[2], Calisir M.[2]

[1]Kandilli Observatory and Earthquake Research Institute, Bogazici University, 34684 Istanbul,Turkey; ozguc@boun.edu.tr

[2]Department of Space Science and Technologies, Akdeniz University Faculty of Science, 07058, Antalya, Turkey; alikilcik@akdeniz.edu.tr; muhammed.calisirr@gmail.com

Abstract

On the basis of a temporal analysis of yearly values of the 10.7 cm solar radio flux (F10.7), the maximum coronal mass ejection (CME) speed index (MCMESI), interplanetary magnetic field strength (scalar B), the solar wind speed, cosmic ray intensity and the geomagnetic Ap, Dst and AE indices, we point out the particularities of solar and geomagnetic activity during the last Solar Cycle (Cycle 24). We also analyze the temporal offset between the F10.7 and the above-mentioned solar, geomagnetic, cosmic and interplanetary indices. It is found that this solar activity index, analyzed jointly with interplanetary parameters, cosmic ray intensity, and geomagnetic activity indices, shows a hysteresis phenomenon. It is observed that these parameters follow different paths for the ascending and descending phases of Cycle 24. The hysteresis phenomenon represents a clue in the search for physical processes responsible for linking the solar activity to near-Earth and geomagnetic responses.

Keywords: 10.7 cm solar radio flux; Solar and geomagnetic activity indices; Solar cycle 24; Hysteresis phenomenon.

Introduction

The dynamic nature of solar activity has profound effects on Earth's environment, making it a critical area of study in solar-terrestrial physics. Solar activity is characterized by various indices, including the 10.7 cm solar radio flux (F10.7), which measures the Sun's radio emission and correlates with the level of solar activity (Barbieri & Mahmot, 2004). Another significant indicator is the maximum coronal mass ejection (CME) speed index (MCMESI), which highlights the power of CMEs, explosive events that eject solar material into space. These solar phenomena influence the interplanetary magnetic field (IMF), solar wind speed, cosmic ray intensity, and geomagnetic indices such as Ap, Dst, and AE.

Solar Cycle 24 (December 2008 - December 2019) exhibited unique characteristics, particularly its notably low solar activity. This cycle presents an invaluable opportunity to explore the interrelationships among various solar, geomagnetic, cosmic, and interplanetary parameters. The cyclic nature of solar activity influences the frequency and intensity of solar flares, CMEs, and other solar events that directly impact Earth's geomagnetic field (Hathaway et al., 2002; Özgüç et al., 2022).

The study of these interactions has shown that geomagnetic activity, measured through indices like Ap, Dst, and AE, is closely related to solar activity (Verbanac et al., 2011; Sarp & Kilcik, 2018). These geomagnetic indices help quantify the effects of solar phenomena on Earth's magnetic environment, illustrating how solar activity drives geomagnetic responses (Obridko & Shelting, 2009; Kirov et al., 2013).

A phenomenon of particular interest is hysteresis, where solar and geomagnetic parameters exhibit different behaviors during the different phases of a solar cycle. This behavior provides insights into the physical processes that link solar activity to geomagnetic effects (Demetrescu

& Dobrica, 2008). Understanding these relationships is crucial for improving our ability to predict space weather events and mitigate their impacts on technological systems and human activities on Earth.

In this study, we analyze the temporal variations, cross-correlations, and hysteresis patterns of the 10.7 cm solar radio flux, MCMESI, scalar B, solar wind speed, cosmic ray intensity, and geomagnetic indices during Solar Cycle 24. By examining these parameters, we aim to elucidate the complex interactions between solar and geomagnetic activity and contribute to the broader understanding of solar-terrestrial relationships. Data and methods are detailed in Section 2, results are presented in Section 3, and conclusions is provided in Section 4.

Data

This study uses datasets covering Solar Cycle 24 (December 2008 - December 2019) to analyze solar and geomagnetic activities. The data and their sources are detailed below:

i) 10.7 cm Solar Radio Flux (F10.7): The solar radio flux at 10.7 cm (2800 MHz) is an excellent indicator of solar activity. Often called the F10.7 index, it is one of the longest running records of solar activity. The F10.7 radio emissions originates high in the chromosphere and low in the corona of the solar atmosphere. It correlates well with the sunspot number as well as a number of UltraViolet (UV) and visible solar irradiance records. The F10.7 has been measured consistently in Canada since 1947, first at Ottawa, Ontario; and then at the Penticton Radio Observatory in British Columbia, Canada. Unlike many solar indices, the F10.7 radio flux can easily be measured reliably on a day-to-day basis from the Earth's surface, in all conditions of weather. Therefore, it is a very robust data set with few gaps due to the calibration issues.

ii) Maximum Coronal Mass Ejection Speed Index (MCMESI): It introduced by Kilcik A, et al., (2011) as a new solar and geomagnetic activity index as a measure of the linear speed of the fastest CME observed in a day. The MCMESI displays better correlation with geomagnetic indices than the ISSN, which suggests that the MCMESI may be a powerful indicator of both solar and geomagnetic activity (Kilcik et al., 2011).

iii) Interplanetary Magnetic Field (IMF)/Scalar B: It includes solar magnetic fields that were carried into interplanetary space by the solar wind. The source of the fast solar wind is thought to be coronal holes, which are open magnetic-field regions on the Sun, while slow solar wind originates at closed magnetic regions thought to be associated with active regions. The structure and dynamics of the IMF (scalar B) are key for understanding space weather.

iv) Solar Wind Speed: The solar wind continuously flows outward from the Sun and consists mainly of protons and electrons in a state known as a plasma. Solar magnetic field is embedded in the plasma and flows outward with the solar wind. Different regions on the Sun produce solar wind of different speeds and densities. Coronal holes produce solar wind of high speed, ranging from 500 to 800 Km/s. The north and south poles of the Sun have large, persistent coronal holes, so high latitudes are filled with fast solar wind. In the equatorial plane, where the Earth and the other planets orbit, the most common state of the solar wind is the slow speed wind, with speeds of about 400 Km/s. High speed winds bring geomagnetic storms while slow speed winds bring calm space weather condition.

v) Cosmic-Ray Intensities (CRI): Cosmic rays are high energy particles that flow into our solar system from outer space. The intensity at which cosmic rays collide with the Earth's atmosphere varies. It varies also with latitude, because the flux is modulated by the Earth's magnetic field and cosmic rays are guided by the Earth's magnetic field lines. The cosmic ray intensity also varies with altitude. The corrected cosmic ray intensity data used in this study are taken from Oulu/Finland nötron monitor station (https://cosmicrays.oulu.fi/#solar)

vi) Geomagnetic Ap Index: The K index is used to measure changes in the horizontal component of the magnetic field. However, since the K index is not directly related to geomagnetic activity the Kp index was introduced and it is derived from the mean standardized K index of 13 geomagnetic observatories located between ± 44 and ± 60 degrees of the geomagnetic latitude. This planetary index is designed to measure the magnetic effect of solar particle radiation. The 3-hourly ap index is derived from the Kp index and the Ap index used in this study is an average of the ap index over 24 hours (Bartels, Heck, and Johnston, 1939).

vii) Geomagnetic AE (Auroral Electrojet) Index: AE index is designed to provide a global, quantitative measure of auroral zone magnetic activity produced by enhanced Ionospheric currents flowing below and within the auroral oval. Ideally, It is the total range of deviation at an instant of time from quiet day values of the horizontal magnetic field (h) around the auroral oval. Defined and developed by Davis and Sugiura [1966], AE has been usefully employed both qualitatively as a correlative index in studies of substorm morphology, the behavior of communication satellites, radio propagation, radio scintillation, and the coupling between the interplanetary magnetic field and the earth's magnetosphere. AE data is maintained at WDC (World Data Center) Kyoto and NGDC (National Geophysical Data Center).

viii) Geomagnetic Disturbance Storm Time Index (Dst): It was proposed by Sugiura (1964) to measure the magnitude of magnetospheric currents that produce an axially symmetric disturbance field. This index is a measure of the variation of the field due to the ring current arising in the magnetosphere during a geomagnetic storm. Data from four observatories are used to derive the Dst index. Because of the need for good data, these observatories were chosen sufficiently far from the auroral and equatorial electrojet regions. Irregularities observed in the Dst index that have a negative sign and fluctuate within the -50 nT $\leq$ Dst < -30 nT range are called small storms, while those within the -100 nT $\leq$ Dst < -50 nT range are called moderate storms, -200 nT $\leq$ Dst < -100 nT fluctuations are called intense storms, and a Dst index below -250 nT defines big geomagnetic storms (Gonzalez, Tsurutani, and Clúa de Gonzalez, 1999).

Method and Results

Temporal Variation Analysis

As a first step, we plot the temporal variation of used data sets (Figure 1 and Table 1). To remove the short-term fluctuations all monthly mean data sets were smoothed with 11 step running average smoothing method.

Figure 1. *Temporal variation analysis of the relationship between F10.7 and other indices.*

Table 1. *Results of temporal variation analysis*

Data	**Maximum Values**		**Delay between peaks (month)**
F10.7-Scalar B	145.35	6.9	6
F10.7-Dst	145.35	-21.12	10
F10.7-Ap	145.35	12.48	12
F10.7-CRI	145.35	6103.29	7
F10.7-Solar Wind Speed	145.35	467.42	28
F10.7-AE	145.35	220.33	12
F10.7-MCMESI	145.35	552.57	– 27

Cross Correlation Analysis

As a second step, we performed cross correlation analysis between F10.7 and other indices used (Figure 2 and Table 2). The method gives the maximum correlation between two data sets together with possible time delay. If the delay is negative that means the first parameter leads the second one and vice versa. The error level of obtained correlation coefficients were calculated by using Fisher's test that gives the upper and lower boundary of the correlation coefficient with 95 % confidence level.

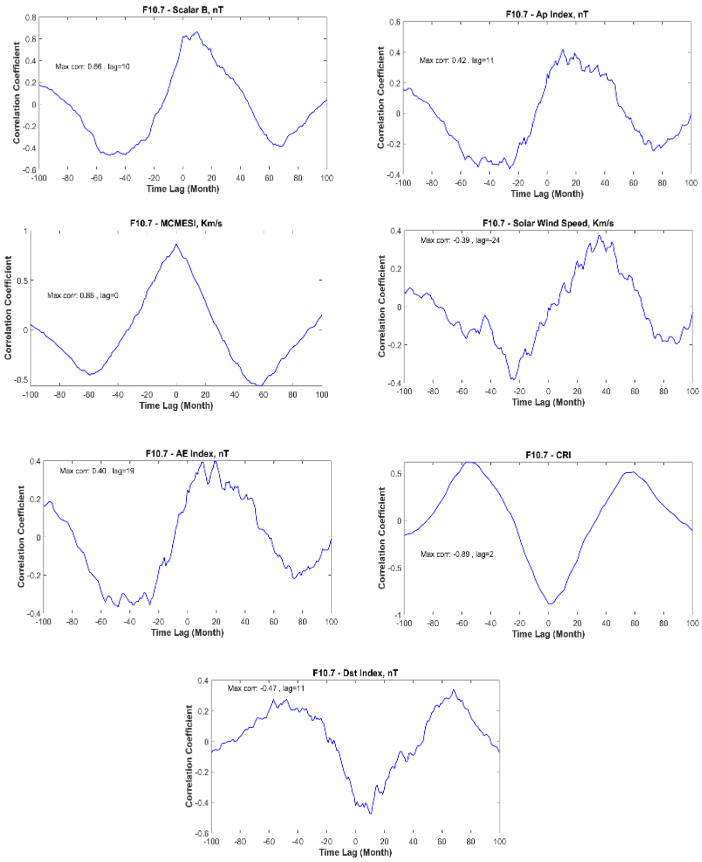

Figure 2. *Cross-correlation analysis results between F10.7 and other indices.*

Table 2. *Results of cross correlation analysis*

Data	**Correlation Coefficient**	**Time Lag**
F10.7-Scalar B	0.66 ± 0.07	10
F10.7-MCMESI	0.86 ± 0.04	0
F10.7-Dst	-0.47 ± 0.08	11
F10.7-AE	0.40 ± 0.08	19
F10.7-Solar Wind Speed	-0.39 ± 0.08	-24
F10.7-Ap	0.42 ± 0.08	11
F10.7-CRI	-0.89 ± 0.04	2

Hysteresis Analysis

As a last step of our analysis, we plotted the hysteresis behavior between the solar radio flux (F10.7) and the maximum (CME) speed index (MCMESI), Cosmic ray intensity (CRI), solar wind speed, Disturbance Storm Time (Dst) index, interplanetary magnetic field (IMF)/Scalar B, and geomagnetic Ap / AE index during solar cycle 24 (Figure 3). We choose the F10.7 solar activity index to be the abscissa of the plots with the equal scale in below figures to display the effects of hysteresis clearly. In general, all data sets show hysteresis behavior only around the maximum phase of the Cycle 24. Dst and CRI data sets show counter clockwise circulation, while the Scalar B, the MCMESI, Ap Index, Solar wind speed and AE index show clockwise circulation which is not a normal characteristic of hysteresis in magnetic materials.

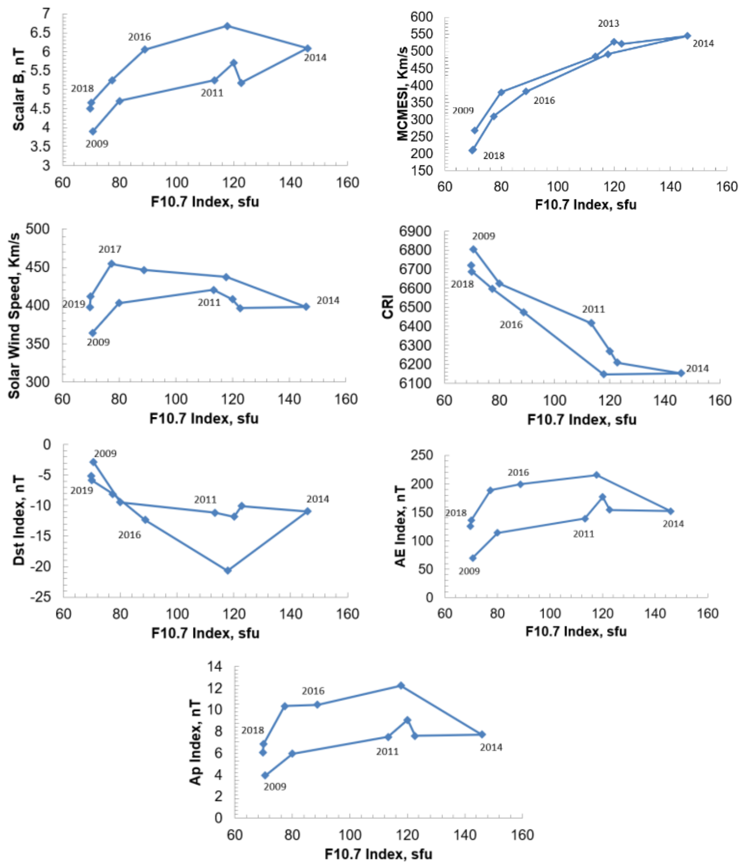

Figure 3. *The hysteresis behavior between the solar radio flux (F10.7) and the MCMESI, CRI, solar wind speed, Dst index, IMF/Scalar B, and Ap, AE index during solar cycle 24.*

Conclusion

We examined the relationship between solar, cosmic and geomagnetic activities during the last Solar Cycle (Cycle 24) on the basis of a temporal analysis, correlation coefficient calculations and hysteresis phenomena. Our main findings are as follows;

- In general, all data sets show hysteresis behavior only around the maximum phase of the Cycle 24. Dst and CRI data sets show counter clockwise circulation, while the Scalar B, the MCMESI, Ap Index, Solar wind speed and AE index show clockwise circulation which is not a normal characteristic of hysteresis in magnetic materials.

- It is observed that these parameters follow different paths for the ascending and descending phases of Cycle 24.
- The hysteresis phenomenon represents a clue in the search for physical processes responsible for linking the solar activity to near-Earth and geomagnetic responses.
- We analyzed the temporal offset between the F10.7 and the above-mentioned solar, geomagnetic, cosmic and interplanetary indices. We found that the peak of all parameters except the MCMESI show time delay with F10.7 and all data sets used here show meaningful correlation with F10.7.

References

Barbieri, L.P. and Mahmot, R.E. 2004, October–November 2003's space weather and operations lessons learned, Space Weather 2, S09002

Bartels, J., N. H. Heck, and H. F. Johnston (1939), The three-hour-range index measuring geomagnetic activity, Terr. Magn. Atmos. Electr., 44(4), 411–454, doi:10.1029/TE044i004p00411.

Davis, T. N., and M. Sugiura (1966), Auroral electrojet activity index AE and its universal time variations, J. Geophys. Res., 71(3), 785–801, doi:10.1029/JZ071i003p00785.

Demetrescu, C., Dobrica, V. (2008), Signature of Hale and Gleissberg solar cycles in the geomagnetic activity. JGRA, Vol 113, Issue A2, CiteID A02103, DOI:10.1029/2007JA012570

Gonzalez, W.D., Tsurutani, B.T. & Clúa de Gonzalez, A.L. Interplanetary origin of geomagnetic storms. Space Science Reviews 88, 529–562 (1999). https://doi.org/10.1023/A:1005160129098

Hathaway, D. H., Wilson, R. M., Reichmann, E. J.(2002). Group Sunspot Numbers: Sunspot Cycle Characteristics, Sol. Phys. 211, 357 – 370.

Kilcik, A., Yurchyshyn, V. B., Abramenko, V., Goode, P. R., Gopalswamy, N., Ozguc, A., & Rozelot, J. P. (2011a). Maximum coronal mass ejection speed as an indicator of solar and geomagnetic activities. The Astrophysical Journal, 727(1), 44.

Kilcik, A., Yurchyshyn, V. B., Abramenko, V., Goode, P., Ozguc, A., Rozelot, J. P., & Cao, W. (2011b). Time distribution of large and small sunspot groups over four solar cycles, The Astrophysical Journal, 730, 30–37.

Kirov, B., Obridko, V. N., Georgieva, K., Nepomnyashtaya, E. V., Shelting, B. D. (2013). Long-term variations of geomagnetic activity and their solar sources, Geomagnetism and Aeronomy, Vol 53, Issue 7, pp.813-817, DOI:10.1134/S0016793213070128

Obridko, V. N., Shelting, B. D. (2009). Anomalies in the evolution of global and large-scale solar magnetic fields as the precursors of several upcoming low solar cycles, Astronomy Letters, Vol 35, Issue 4, pp.247-252, DOI:10.1134/S1063773709040045.

Ozguc, A., Kilcik, A., Yurchyshyn, V. (2022). Temporal and Periodic Variations of the Solar Flare Index During the Last Four Solar Cycles and Their Association with Selected Geomagnetic-Activity Parameters, SolPhys, Vol 297, Issue 9, article id.112, DOI:10.1007/s11207-022-02049-7.

Sarp, V., Kilcik, A. (2018). Solar flare and geomagnetic activity relations, Turkish Journal of Physics, Vol 42, Issue 3, pp. 283-292, DOI:10.3906/fiz-1712-18.

Sugiura, M. (1964) Annals of the International Geophysical Year, Vol. 35. Pergamon Press, Oxford. 945.

Verbanac, G., Mandea, M., Vrsnak, B., Sentic, S. (2011), Evolution of solar and geomagnetic activity indices, and their relationship: 1960 – 2001. SolPhys. Issue 1-2, pp. 183-195, DOI:10.1007/s11207-011-9801-y.